

# Assessment of gas permeability through porous skeletal media with anisotropic internal structure

Grzegorz Wałowski<sup>1</sup>, and Gabriel Filipczak<sup>2,\*</sup>

<sup>1</sup>Institute of Technology and Life Sciences, Renewable Energy Department, Biskupińska Street 67, 60-463 Poznań, Poland

<sup>2</sup>Opole University of Technology, Faculty of Mechanical Engineering, Department of Process Engineering, Mikołajczyka Street 5, 45-271 Opole, Poland

**Abstract.** The results of experimental studies in the field of gas permeability of porous materials referring to gas flow have been shown. Coal chars with anisotropic porous-slotted structure have been tested. The studies have been carried out on a special test bench that allows for the measurement of gas permeability in terms of three flow orientations related to symmetrical specimens in the cubic form. The results of the measurements indicate that there is a considerable effect of the flow directivity on the permeability of carbonizers, which results from their integral anisotropic structure. A permeability coefficient for such materials has been defined and the experimental assessment of the value of this coefficient against gas flow and the total pressure drop on a porous medium has been made. The usefulness of computation methods characterising the hydrodynamics of gas flow through porous materials has been made, and the possibility of a numerical mapping of the flow geometry of solid materials with tortuous structure has been indicated.

## 1 Introduction

Gas flow through media with porous structures takes place in many process areas. It is most often associated with filtration or gas flow through filling layers as a porous medium with a loose composition. This type of flow is also included in the technological processes involving the thermal processing of coal and also during the migration of natural gas (e.g. methane) through natural formations, or the flow of reactive gas through various kinds of coal char, such as coke, activated carbon etc. [1-3]. In some technological processes, the operation of apparatus occurring in them depends on the type and design of gaseous phase dispensers, which are very often made from porous materials [4, 5].

In each case, the recognition of gas flow conditions through a porous media carries significant problems with the description of hydrodynamics and the assessment of the mechanism of gas flow through porous media, especially in the context of their varied internal structure. On the other hand, the knowledge of these mechanisms allows us to assess the process conditions associated with hydrodynamics of gas flow through such types of material, and, consequently, the detailed description of hydrodynamic phenomena accompanying the flow of gas through porous media.

Despite the widespread presence of gas flow in porous materials, in the literature on this area there is still a lack of an unequivocal interpretation and a clear indication of the nature of the hydrodynamic phenomena accompanying this flow. The main reason for this is seen

in the very complex and diverse structure of porous materials, which due to the variable flow conditions entails many difficulties in describing these phenomena, but very often also due to the varying scale of the process - from the porous solid grain to the porous layer bed. Although a literature does not lack models that incorporate structural features of porous materials in its description, especially in terms of homogenization theory [6-9], the problem of the influence of the anisotropic structure on permeability of porous materials is still not sufficiently recognized. This situation becomes even more complicated with respect to the hydrodynamics assessment of gas flow through backbone (skeletal) porous materials. At the same time, it is difficult to find information concerning the hydrodynamics of gas flow through such kinds of porous materials. An exemplary comparison of some literature position [10-18] referring on hydrodynamics of gas flow through selected porous beds is characterized in Table 1.

The scope of this work involves the presentation of the investigation results in the field of gas permeability through porous material with skeletal structure. Experimental results have been reported and gas permeability assessment of various kinds of solid (backbone) porous materials has been made. Evaluation of process conditions related to hydrodynamics of gas flow through porous materials with an anisotropic internal structure is carried out. Additionally, the possibilities of numerical modelling techniques to describe the flow structure of porous materials with a skeletal structure are also demonstrated.

\*Corresponding author: [g.filipczak@po.opole.pl](mailto:g.filipczak@po.opole.pl)

**Table 1.** Selected studies referring to investigations upon hydrodynamics of gas flow through porous media.

Author	Kind of gas	Deposit characteristics				
		Kind of material	Deposit height $H$ , m	Mean diameter of deposit $D$ , m	Equivalent diameter of grain / pores $d_e$ , m	Porosity of sample / deposit $\varepsilon$
Blicharski et. al. [10]	air	rock	0.0254	0.0254	-	0.49
Brauer [11]	air	formed spheres of uniform size	0.50	-	0.0024	0.32
Dyga, Płaczek [12]	air	aluminium foam, 20PPI	1.00	0.020	0.00345	0.93
Ergun [13]	CO <sub>2</sub> , N <sub>2</sub> , CH <sub>4</sub> , H <sub>2</sub>	coke	0.95	0.724	-	0.42
Hehlmann [14]	air	fine coke	0.20	-	0.0049	0.61
Mertas et al. [15]	N <sub>2</sub>	coke yielded grains	0.08	0.020	-	-
Skotniczy [16]	air	glass balls	0.04	0.110	0.0050	-
Warpechowski, Jopkiewicz [17]	air	coke	0.95	0.380	0.0330	0.42
Wong et al. [18]	air	biochar with clay	0.07	0.070	$3 \cdot 10^{-6}$	0.10

## 2 Quality of process conditions

Porous medium is characterised by a given porosity and its flow structure depends not only on this porosity, but also on the size (diameter) of tubules (pores) and their shape - at the given length of the pore. Another specific feature of porous materials is associated with their ability to store and transport of fluids as the results of internal and external forces. A study by Aksielrud and Altszuler [19] contains a statement that gas flow through porous media with the pores size of millimetres and less is dominated by the process phenomena resulting from the flow hydrodynamics of viscous fluid whereas in flows through structures with a very small pore size, e.g. tenths of a micrometre, these phenomena are restrained by the physiochemical and diffusive mechanism influences that take place at their interface.

This is confirmed by other studies [20, 21], where the disparity between these phenomena decreases in the conditions when a high intensity of gas movement is maintained. Nonetheless, in each case, the gas flow mechanism is closely related to the geometric structure of porous layer. Therefore, it depends on the configuration and the pore size, as well as on their shape and sinuosity. In the general assumption, two major cases of fluid flow in porous media could be distinguished, as it is shown in Fig. 1. The first one occurs for the case of the flow through a grained layer, while the other one concerns a porous material with a solid (skeletal) structure with empty pores.

The first case (Fig. 1a) involves the flow in the space between the grains and we can assume that the space resulting from the porosity of packed bed layer ( $\varepsilon$ ) is completely available for the fluid flow. Whereas, in the second case (Fig. 1b), the flow occurs only in the area of the pores and channels of open and interconnected, with a surface of flow much smaller than that required by absolute porosity of the material.

An additional complexity of hydrodynamics stems from the fact that skeletal structures are compact (rigid) deposits that are not able to be relaxed during pressure increase in the system. As a consequence, the flow conditions through such structures will be different from each other and the flow deviation will be greater than greater the porous sinuosity and content of closed or blinded pores. Lambe and Whitman [22], among others, point out that the measure of this deviation can be coefficient of pressure drop which value corresponds to the bed porosity ( $\varepsilon$ ), the hydraulic diameter of the pores ( $d_e$ ), and the really flow path ( $L_e$ ), which results from the sinuosity of the tubular pores.

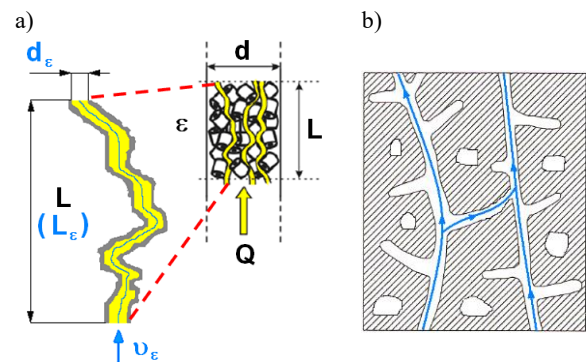


**Fig. 1.** Flow scheme through a porous bed: a) grain layer with a tortuous channels [22]; b) rigid skeletal structure with open flow channels and blind pores and closed for the flow [23].

The basis for a detailed analysis of fluid flow in porous media is still Darcy law. In its original form, this law describes the conditions for permeability of various kinds of grained bed by reference to the filtration mechanism during laminar flow of water through a sand layer, which constitutes a model grained medium (Fig. 1a). If the variability of liquid properties is take into account, the velocity through a porous bed will be

proportional to the change in density ( $\rho$ ) and inversely proportional to the change in viscosity ( $\eta$ ). Then the Darcy equation describing the permeability ( $Q$ ) of the porous bed takes the following formula

$$Q = K A_o \frac{\rho g \Delta h}{\eta L} \quad (1)$$

where  $\Delta h$  denotes pressure drop,  $L$ - height of porous medium,  $A_o$ - layer bed cross-section and  $g$ - gravitational acceleration.

This formula remains one of the characteristics of the contemporary description of this phenomenon, although it refers (from definition) only to laminar flow.

The  $K$  coefficient in equation (1) describes the so-called permeability of a porous medium, and its value, as shown by the Darcy model, is characteristic of a given porous medium. Since this coefficient (by definition) has a surface dimension, its value from a hydrodynamic point of view – as characteristic dimension – is very often considered as a certain geometric feature that characterizes the total permeability of the porous material. On the other hand, the value of such permeability depends not only on filtration characteristics of the porous medium (its structure, particle size, their density, porosity etc.), but also on the physical properties of fluid, especially its viscosity. As a rule, this factor does not depend on the shape and size of the bed itself.

Of course, the Darcy model also applies to the description of pressuring flows. Then for equation (1) we will get

$$Q = K A_o \frac{\Delta P}{\eta L} \quad (2)$$

Therefore

$$K = \eta \frac{Q}{A_o} \frac{L}{\Delta P} \quad (3)$$

The last equation shows that for a given volumetric flow rate ( $Q$ ) the permeability of a porous bed could be determined by means of experiments if the fluid properties ( $\eta$ ) and the geometrical parameters of the flow system ( $A_o$ ) are known. The pressure drop on the bed is then experimental value.

From physics phenomena point of view, the permeability of the porous medium can be subordinated to various hydrodynamic criteria, depending on the structure of the medium, the type of fluid (single- and multi-phase) and the method of flow forced (gravity, pressuring).

Numerous publications in this respect [1, 23, 24-27], describing this process both from the research and analytical side, *de facto* relates to the filtration phenomenon and are generally associated with the laminar flow of liquids through a granular bed, according to Darcy's law [28]. Naturally, this does not exhaust the many other cases of fluid flow through porous media. For example, for the transitional and turbulent liquid flow Forchheimer study can be

distinguished [29-30] or Ergun [13] and Brinkman's research [31]. A more advanced description of flow for a spatial system of capillaries in the form of a bundle of sinuous tubules may be found in the studies by Kozeny-Carman [1, 32].

A characteristic comparison between the ranges of the applicability of Darcy, Forchheimer and Brinkman models is shown in Figure 2, which taken from the Hansen study [33] From the sequence of function describing the gas permeability versus a pressure drop in a porous medium it follows that outside of the Darcy area (A) where for laminar flow linear dependence of this function exists, in other areas referring to the transitional and turbulent flow (B and C), this function is nonlinear. In addition, if fluid motion is influenced only by the diffusion phenomenon (close to the smallest permeability value), in the laminar region the description of the permeability is also nonlinear. It follows that the greater turbulence of flow, the inertia forces has a more significant effect on flow resistance. The scope of applicability of the fundamental models for the granular layers resulting from these premises relative to the Reynolds number is characterized in Table 2.

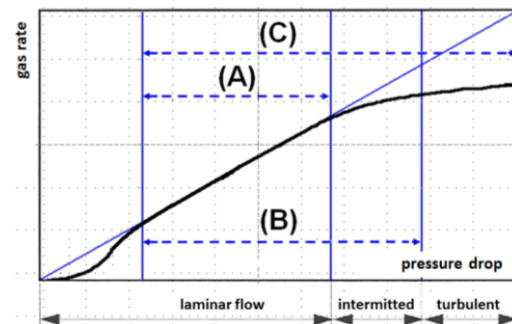


**Fig. 2.** General characteristics of flow conditions through porous beds: (A) - Darcy area, (B) - Forchheimer area, (C) - Brinkman area, acc. [33].

**Table 2.** The scope of significance of flow models through granular layers, acc. [29, 30].

Hydrodynamics models			
laminar flow		intermitted	turbulent
Re<1-3	3<Re<15	15<Re<120	Re>120
pre-Darcy area	Darcy law		
	Forchheimer formula		
	Brinkman formula		

In each case, the Reynolds number is determined by the equivalent diameter ( $d_e$ ) of flow channels and the mean fluid velocity ( $v_f$ ) in these channels, according to equation

$$Re = \frac{v_f d_e \rho_f}{\eta_f} \quad (4)$$

An exemplary comparison of a few characteristic models used in the calculation of the coefficient of permeability for different beds is shown in Table 3.

It is evident that these models are very varied and in many cases are far from Darcy assumptions, and very often – like to Slichter and Dullien models – do not take

into account the fluid properties. Not all of them, such as ASTM and Szczelkaczew, take into account the porosity parameter as a characteristic feature of each porous material. On the other hand, there is no reference to porous skeletal (rigid) structures, which considerably limits the possibility of using these types of models to describe hydrodynamics of gas flow through porous skeletal forms. The self-made tests are described below.

### 3 Experimental studies and analysis of measurement results

The tests on permeability of porous materials were carried out for a many different types of material, for which the average porosity was within the limits (22-56) %. Most of them were coal chars (cokes) derived from miscellaneous thermal processing of bituminous coal, and materials such as partially melted gangue (including volcanic rock), natural and synthetic pumice, and porous polyamide with symmetrical spatial structure.

The tested materials were different in structure and their internal form was evaluated on the basis of a scanning image – Fig. 3. Based on the following, the porosity of each material was determined and its effective value resulting from the openings of the pores.

Experimental studies were carried out on a specially designed set-up that is currently being patented [37]. An essential element of this measuring system is a flow module (Fig. 4a), in which a specimen of porous material (1) is placed.

The specimens were cube shaped (Fig. 4b), and the module flow channel design allowed for the measurements of permeability for each of the three main

flow directions (X, Y, Z) by rotating the cubic specimen in a selected plane of the measuring cell.

Experimental set-up was equipped with a rotameter to measure of gas flow and two pressure gauges for assessment of pressure drop (at known temperature of gas). For a measuring of permeability a gas volume flow rate was assumed, resulting from allowable pressure drop on the porous specimen. Of course, the scope of research included also determination of the apparent density of porous deposits as well as the overall porosity of each tested specimen.

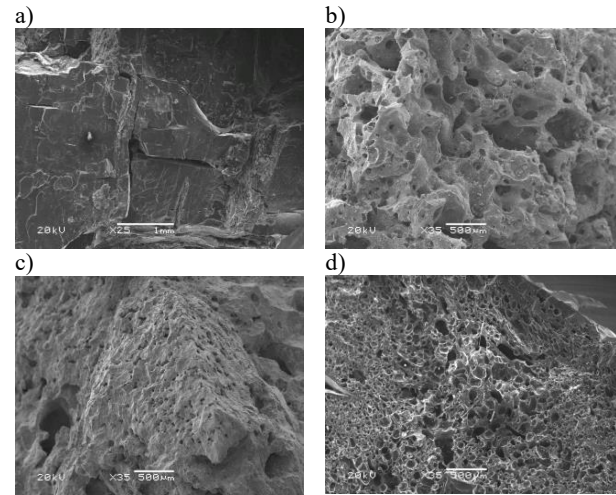


**Fig. 3.** Exemplary SEM images of the coal char specimen forms: a) *in situ* coal char, b) coke, c) *in situ* gangue, d) *ex situ* coal char (x35 zoom).

**Table 3.** Coefficient of permeability in the assessment of various research sources.

Author	Model	Remarks
ASTM ( <i>American Society for Testing and Materials</i> ) [34]	$K_{ASTM} = \frac{2\eta L Q_g P_{wyl}}{A_o (P_{wl}^2 - P_{wyl}^2)} = \frac{\eta L Q_g P_{wyl}}{A_o \Delta P_{zm}} \frac{2}{(P_{wl} + P_{wyl})}$	oil and gas sands and shales
Brinkman, [33]	$K_B = \frac{v_o \eta}{\frac{\Delta P}{L} - (\rho \beta v_o^2) - \eta v_o}$	air cooling of packed fruit
Darcy [23, 28]	$K_{Da} = \frac{v_o \eta L}{\Delta P_{zm}}$	sand-ground (water)
Dullien [23]	$K_{Du} = \frac{d_e^2}{180} \left( \frac{\varepsilon^3}{(1 - \varepsilon)^2} \right)$	granular materials
Ergun [13]	$K_E = \frac{1}{4} \left( \frac{1,75 \rho_f v_o^2}{\sqrt{150} \sqrt{\varepsilon^3}} \frac{L}{\Delta P} + \sqrt{\left( \frac{1,75^2 \rho_f v_o^4}{150 \varepsilon^3} \frac{L^2}{\Delta P^2} \right) + \left( 4 v_o \eta \frac{L}{\Delta P} \right)} \right)^2$	pressure drop in gas flow
Forchheimer [30, 33]	$K_F = \frac{v_o \eta}{\frac{\Delta P}{L} - (\rho \beta v_o^2) + C}$	granular and porous materials
Slichter [35]	$K_S = 7,8 \varepsilon^{3,26} d_c^2$	symmetrical spherical bed (gas)
Szczelkaczew [36]	$K_{Sz} = \frac{v_o \eta}{\hat{g} \rho}$	grained medium - flow through a straight pipe (fluid)

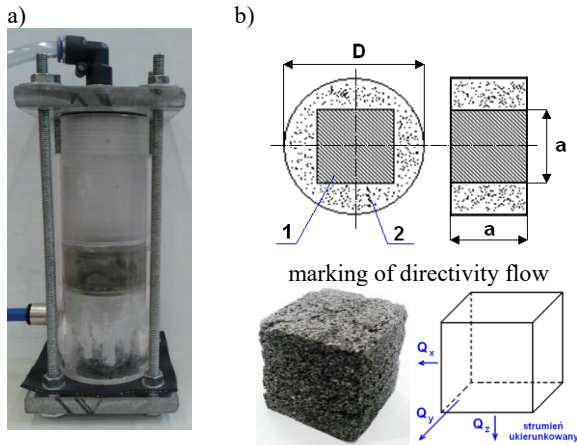


**Fig. 4.** Gas permeability meter: a) flow module channel, b) measurement cell: 1- specimen of porous material, 2- sealing frame with diameter ( $D$ ) and the size of the sample ( $a$ ).

An example of measurement results characterizing the permeability ( $Q$ ) of the char *in situ* versus pressure drop ( $\Delta P_{zm}$ ) on the porous bed are shown in Fig. 5. From distribution of experimental points it can be seen that the permeability of this kind of material depends significantly on the direction (X, Y, Z) of gas flow. This indicates a distinct asymmetry of permeability flow rate to a given flow direction and consequently to the apparently anisotropic structure of the material to which the permeation tensor is an anisotropic tensor. Similar results have also been obtained for other such materials.

The point of reference for such asymmetry may be a porous polyamide which is a material with spherical sintered bed of particles with a diameter of approximately 0.1 mm. The experimental data presented in Fig. 5b show that the polyamide permeability characteristics are practically independent of the flow direction of the gas, which indicates the symmetrical structure of the polyamide. At the same time, despite a significantly lower porosity than carbonate *in situ*, this polyamide is characterized by similar gas flow characteristics. These results confirm the perception that higher permeability of coal char results more from their porous-slit structure than from porosity scale.

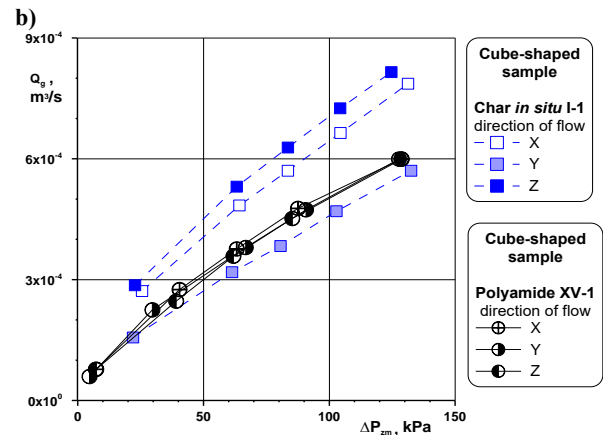
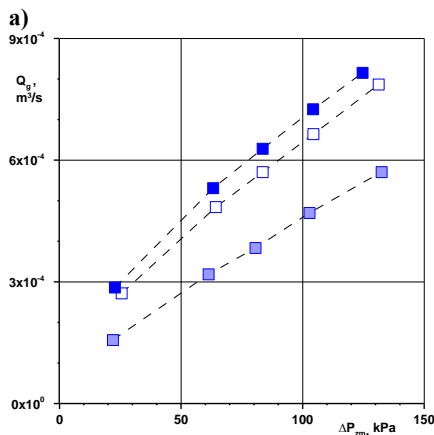


**Fig. 5.** Experimental points characterizing asymmetric flow of air through a deposit of carbonate *in situ* (a) and comparison of this asymmetry to sintered polyamide (b); cubic shape sample with dimension  $a=20$  mm.

It is interesting to note that for the porous polyamide the permeability characteristics are also non-linear, which in the scope of conducted measurements proves the advantage of the turbulent gas flow.

This is confirmed by experiment results shown in Fig. 6, which characterize the gas permeability of coke with a multiplied volume of cubic specimen –  $a=30 \times 30 \times 30$ ,  $40 \times 40 \times 40$  and  $50 \times 50 \times 50$  mm. Also, the results of these measurements show that the “reciprocal distance” for gas permeability between multiple-volume specimens is not transferred to a proportional displacement of the permeability characteristics. This is very important in terms of geometry scale transfer, and at the same time it confirms the thesis that in case of porous skeletal materials their porosity scale does not form the dominant factor in the description of gas permeability hydrodynamics.

This observation confirms the measurement results shown in Fig. 7, referring to the average permeability of various materials for airflow in two orthogonal directions (Y, Z). In each case (and this is confirmed by the results of studies for other systems – [38]), materials with a relatively large porosity such as pumice or cokes are characterised by a very low permeability, which demonstrates that their internal structure is largely closed for fluid flow.

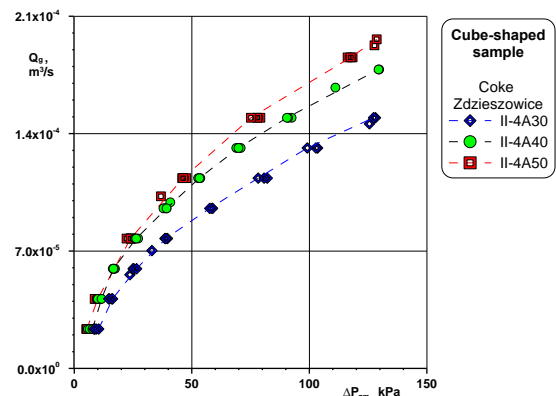


**Fig. 6.** Characteristics of permeability of coke with multiplied specimen size ( $a=30, 40$  and  $50$  mm) – air flow.

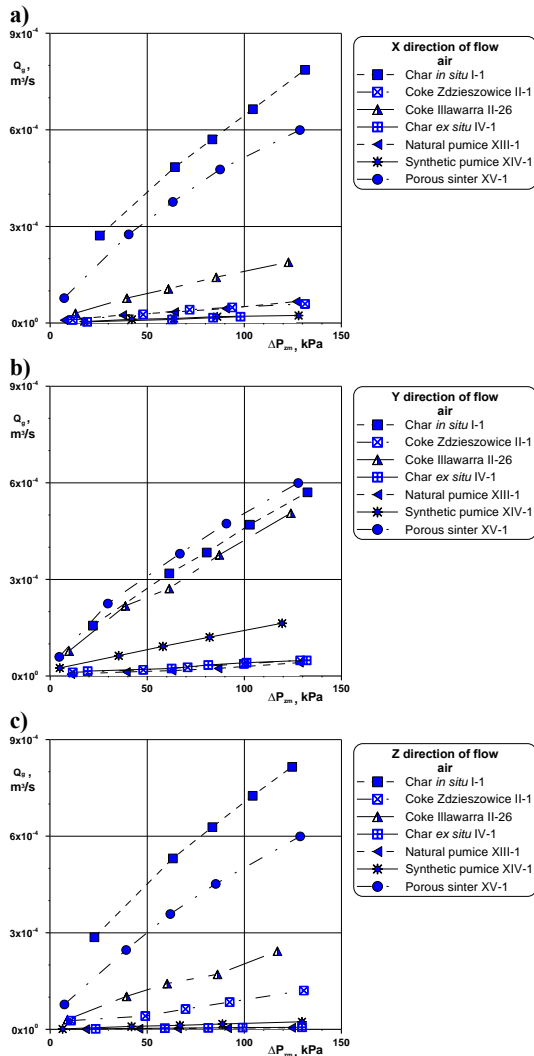


**Fig. 7.** Permeability of porous materials in regard of the gas flow direction: a) flow direction X, b) Y, c) Z.

A comparative statement of calculation value of the permeability coefficient, calculated with respect to the models shown in Table 3, has been illustrated in Fig. 8. As can be seen, in all analysed cases, very different results are obtained, which are characteristic both in terms of the calculation method used and the kind of material. There are three characteristic trends distinguish oneself between the value of the permeability coefficient and the pressure increase: decreasing, unchanging and increasing.

According to Darcy model, declining trend indicates a greater impact of gas choking than it would be by rise the pressure value.

In turn, the apparent trend for Szczelkaczew model results directly from the increase in the calculated gas flow velocity (with its properties), which is proportionally related to the value of this coefficient. Furthermore, by definition of this method, the values of the permeability coefficient also have values much higher than for the other models. In that above context, invariant trends in the values of the permeability coefficient are directly related to the form of the computational models (Tab. 3).

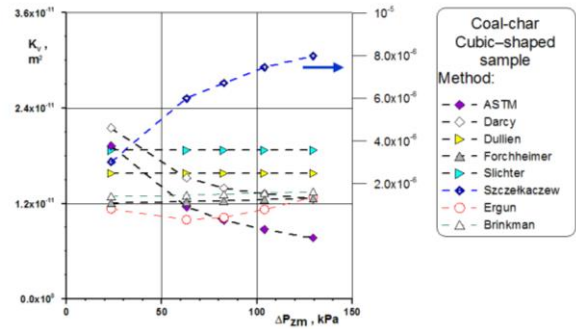


**Fig. 8.** Coefficient of permeability applied to the different calculation methods.

For comparison, on Fig. 9 are presented the results of calculations according to the method of ASTM (Tab. 3), put together for chosen chars from deposits of hard coals in the area of world. These results are pointing for very strong tying together the structure of these chars from of them gas permeability. It proves about distinct anisotropic of this group of porous materials.

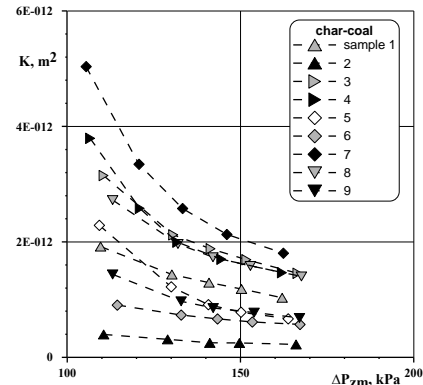


**Fig. 9.** Coefficient of permeability applied to ASTM method (cubic samples): ▲ (1) Czech Republic-a, ▲ (2) Czech Republic-b, ► (3) Australia-a, ► (4) Australia-b, ◊ (5) Poland-a, ◆ (6) Poland-b, ◆ (7) Poland-c, ▼ (8) USA, ▼ (9) Canada.

Due to the great discrepancies and simultaneously in view of numerous limitations in use of models known in the literature, both in the aspect of the structure of porous materials and in the approach to hydrodynamics evaluation of gas flow through such materials, an attempt was made to develop an own model for estimating the permeability coefficient.

From the assumption, definition of model is referred to an alternative approach that results from pressure drop connected with local flow resistance. With reference of the loss coefficient of flow ( $\xi_\varepsilon$ ) and gas velocity ( $v_g$ ) to the conditions associated with the mean porosity value ( $\varepsilon$ ), this could be written as

$$\Delta P = \xi_\varepsilon \frac{\rho_g v_\varepsilon}{2} \quad (4)$$

Transformation of this equation leads to expression

$$Q_g = \sqrt{A_o^2 \frac{2 \Delta P}{\xi_\varepsilon \rho_g}} = \sqrt{\frac{2 A_o^2}{\xi_\varepsilon}} \sqrt{\frac{\Delta P}{\rho_g}} \quad (5)$$

in which the effective surface area of gas flow ( $A_o$ ) results from the material porosity. In terms of the overall cross-section ( $A$ ) of the flow module channel, it yields to  $A_o = \varepsilon A$ .

It can be easily noticed that the component  $\sqrt{\frac{2A_o^2}{\xi_\varepsilon}}$  of equation (5) has a surface dimension, which in hydrodynamic terms allows it to be treated as the equivalent value of the permeability coefficient. Therefore (by definition)

$$K_v = \sqrt{\frac{2A_o^2}{\xi_\varepsilon}} \quad (6)$$

Then, the gas flow rate is described by the following relation

$$Q_g = K_v \sqrt{\frac{\Delta P}{\rho_g}} \quad (7)$$

If the hydrodynamic parameters are known (flow rate, pressure drop, material porosity and type of gas of course), the permeability coefficient value may be determined by means of experiments. Then relationship (7) can be written as

$$K_v = \frac{Q_g}{\sqrt{\frac{\Delta P_{zm}}{\rho_g}}} \quad (8)$$

The coefficient described in this way may be (from definition) used to determine the permeability with respect to each direction of gas flow (X, Y, Z).

In contrast to the some other shown above models (Tab. 3), formula (8) does not include the impact of gas viscosity on the permeability, but it provides an experimental value, and therefore accounts for all features and parameters resulting from the hydrodynamics of gas flow through porous materials.

The exemplary results of the permeability coefficient determined on Eq. (8) for *in situ* coal char are shown in Fig. 10. It is possible to observe the varying intensity of gas flow relative to a given flow direction, indicating a strong anisotropy of this type of material. Similar results were obtained for other carbonates [38].

The characteristic result of the study on the permeability coefficient is the monotonous nature of the change in its value, together with the increase in pressure. This indicates an appropriately proportional increase in permeability with increasing pressure. In relation to well-known models, this effect much better corresponds to the flow phenomena of porous structures. Of course, such a change is equivalent to an increase in the gas stream.

From equation (8), it is also apparent that the increase of the value of permeability coefficient is more caused by the gas stream than relatively pressure drop. This may be facilitated by the slit-porous of coal-char structure and the possible internal volume deformation of such a skeleton. Experimental data confirm that in

context of comparison of the permeability coefficient to other calculation methods (Fig. 8 and 9) the nature of change such defined coefficient much better reflects the mechanism of this phenomenon. On the other hand, as is apparent from the experimental data [38], for many other materials is observed very low permeability, what has its origin in the different structure of these materials, with a relatively high share of blinded pores and channels closed for flow (Fig. 3).

**Errors and statistics.** For all cases the measurement errors are connected with measure of gas flow rate and pressure drop. With the confidence level of 0.99 for flow gauge calibration, the mean relative error for gas flow rate was  $\pm 5.3\%$ . The average error for manometer gauge was  $\pm 8.7\%$ . As a result, the mean estimation error of permeability coefficient is about  $\pm 12\%$  (Fig. 10).

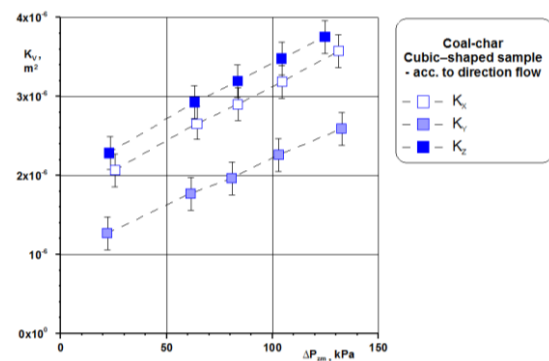


Fig. 10. Gas permeability coefficients for an *in situ* coal char, according to Eq. (8).

### 3.1 Numerical view of skeletal material porosity

Taking into account a very complicated process features of skeletal porous material (including their permeability and anisotropy), an attempt was made to create an integrated area of a tortuous multi-layer network by numerical means. For this purpose there was prepared a relevant simulation algorithm by means of the ANSYS programme, using the so-called Geometry, Mesh and Fluent computational blocks, the details of which are included in other own studies [38, 39].

The analysis included a configuration corresponding to a network of microchannels arranged randomly, when in extreme cases the network channels partially overlapped, creating a quasi-fractal network of curvilinear microchannel (Fig. 11a, b).

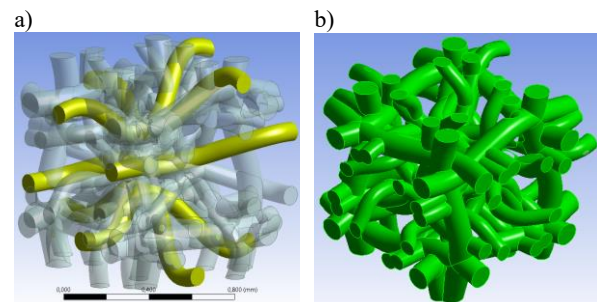
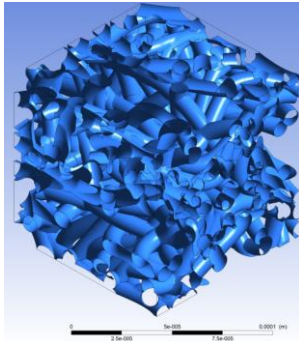


Fig. 11. Modelling of the geometry of microchannel network with curvilinear microchannels (a) and quasi-fractal network of tortuous microchannels (b); a)  $\varepsilon=3.8\%$ , b)  $\varepsilon=39.5\%$ .

On this basis, a fundamental cellular structure as quasi-fractal network of tortuous microcircuits with open for flow pores was modelled, as shown in Fig. 12. This network corresponds to the actual structure of the porous material (Fig. 3), analogous to the quasi-fractal network of tortuous microchannels [39]. Obtained by this way structure model of skeletal porous material allows for further calculations, in accordance with appropriate numerical methods for assessing hydrodynamic of gas flow through such materials.



**Fig. 12.** Numerical projection of structure of the skeletal porous material ( $a=20$  mm,  $d_e=0.123$  mm,  $\varepsilon=54.3\%$ ).

### 3 Conclusions

The recognition of the gas permeability problem of porous media has shown that in literature there is very little information on hydrodynamics of gas flow through solid (skeletal) porous materials. In this respect, appropriate experimental studies of gas permeability of such group of materials have been made, and hydrodynamic phenomena resulting from pressure drop of gas flow have been evaluated. These studies were supplemented with numerical interpretation simulating the internal structure of the materials tested, taking into account the spatial distribution of the flow channels.

It has been found that the scale of permeability of the skeleton porous materials is determined by characteristic parameters such as the size of effective porosity for gas flow and also the anisotropic structure of these materials. Both these quantities have a considerable effect on the permeability coefficient, what was taken into account during the theoretical assessment of the issue.

Based on the local pressure drop a simply model for identification of the permeability coefficient of porous materials is proposed. The investigation results show that such definite coefficient properly reflects trends in the changes of hydrodynamic parameters at gas flow through skeletal porous media.

### References

1. M. Błaszczuk, *Study of migration processes of petroleum substances in porous structures (in Polish)* (PhD Thesis, Łódź University of Technology, 2014)
2. K. Stańczyk at al. *Hydrogen-oriented underground coal gasification for Europe (HUGE). Final report.* (Research Found for Coal and Steel. EUR 25044 EN Project, 2012)
3. P.L. Younger P.L., *Mine Water Environ.* **30**, 127 (2011)
4. M. Sadatomi, *J. Multiphase Flow* **8**, 6, 641 (1982)

5. J.L. Williams, *Catalysis Today* **69**, 3 (2001)
6. J.L. Auriault, T. Strzelecki, J. Bauer, S. He S., *Eur. J. Mech. A/Solids* **9**, 4, 373 (1990)
7. J.L. Auriault J.L., P. Royer, *Soil Mechanics and Porous Media* **3117**, Serie II, 431 (1993)
8. O. Coussy, *Mechanics and Physics of Porous Solids* (John Wiley, 2007)
9. D. Łydźba D., *Studia Geotechnica et Mechanica* **XIII** (3-4), 51 (1991)
10. J. Blicharski, R. Smulski, *AGH Drilling Oil Gas* **29**, 1, 89 (2012)
11. H. Brauer, *Grundlagen der Einphasen- und Mehrphasen Strömungen* (Verlag Sauerländer, 1971)
12. R. Dyga, M. Płaczek, *Inż. Ap. Chem.* **52**, 4, 300 (2013)
13. S. Ergun, *Chemical Eng. Progress*, **48**, 2, 89 (1952)
14. J. Hehlmann at al., *Rocznik Ochrony Środowiska, Koszalin* **11**, 281 (1999)
15. B. Mertas at al., *Karbo* **2**, 163 (2013)
16. P. Skotniczy, *Prace Instytutu Mech. Górniczo-Pan, Kraków*, **10**, 1-4, 103 (2008)
17. K. Warpechowski, A. Jopkiewicz, *Archiwum Odlewnictwa PAN* **2**, 5, 124 (2002)
18. J.T. Wong, Z. Chen, C.W. Ng, M.H. Wong, *Environ. Science and Pollution Research Int.* **23**, 8, 7126 (2016), DOI 10.1007/s11356-015-4871-2
19. G. Aksielrud, M.A. Altszuler, *Mass transfer in porous body (in Polish)* (WNT Warszawa, 1987)
20. G. Dulniew, V. Novikov, *Prociessy pierenosa w nieodnorodnych sriedach.* (Energoatomizdat, 1991)
21. A.P. Mozhaev, *Journal of Engineering Physics and Thermophysics* **75**, 2, 371 (2002)
22. T. Lambe, R.V. Whitman R., *Soil mechanics (in Polish)*, (Arkady, Warszawa 1978)
23. T. Strzelecki at al., *Modelling of flows through porous media (in Polish)* (Wyd. Edukacyjne Wrocław, 2008)
24. A.L. Dullien, *Porous media: fluid transport and pore structure* (Elsevier, 1991)
25. T. Piecuch, *Rocznik Ochrona Środowiska* **11**, 299 (2009)
26. Z. Orzechowski, J. Prywer, R. Zarzycki, *Fluid mechanics in engineering and environmental protection (in Polish)* (WNT Warszawa, 2009)
27. W. Sobieski (Ed.), *Granular porous media (in Polish)* (UW-M Olsztyn, 2016)
28. B. Bębenek, H. Bębenek, *Energy losses in fluid flows (in Polish)* (Wyd. Politechniki Krakowskiej, Kraków 1987)
29. A.M. Amao, *Mathematical model for Darcy Forchheimer flow with applications to well performance analysis* (Master's Thesis, Texas University, Misato, 2007)
30. M. Peszyńska, A. Trykozko, W. Sobieski, *Mathematical Sciences and Applications* **32**, 463 (2010)
31. F. Franchi, B. B. Straughan, *Math. Methods in the Applied Sciences* **19**, 1335 (1996)
32. Z. Kembłowski, *Theoretical basis of chemical and process engineering (in Polish)* (WNT Warszawa, 1985)
33. T.E. Hansen, *Flow in micro porous silicon carbide* (Technical Univ. of Denmark, Copenhagen, 2007)
34. *Standard Test Method for Permeability of Rocks by Flowing Air.* ASME D 4525-90, Reapproved (2001)
35. P. Popielski, *Model of mechanical scouring in terms of the finite element method (in Polish)* (PhD dissertation, Warszawa University of Technology, 2000)
36. S. Pisarczyk, *Soil mechanics (in Polish)* (Politechnika Warszawska, 2005)
37. G. Filipczak, E. Krause, G. Wałowski, Patent PL 225 980
38. G. Wałowski, *Hydrodynamics of gas flow through porous deposits (in Polish)* (PhD Thesis, OUTEch Opole, 2015)
39. G. Wałowski, G. Filipczak, E. Krause, *Modelowanie inżynierskie* **20**, 51, 1236 (2014)